Discovery of an H I Counterpart to the Extended Tail of Mira

L. D. Matthews[1], Y. Libert[2], E. Gérard[3], T. Le Bertre[2], M. J. Reid[1]

ABSTRACT

We report the detection of an H I counterpart to the extended, far-ultraviolet-emitting tail associated with the asymptotic giant branch star Mira (*o* Ceti). Using the Nançay Radio Telescope (NRT), we have detected emission as far as 88′ north of the star, confirming that the tail contains a significant atomic component ($M_{\rm HI} \sim 4 \times 10^{-3}\ M_\odot$). The NRT spectra reveal a deceleration of the tail gas caused by interaction with the local interstellar medium. We estimate an age for the tail of $\sim 1.2 \times 10^5$ years, suggesting that the mass-loss history of Mira has been more prolonged than previous observational estimates. Using the Very Large Array (VLA) we have also imaged the H I tail out to $\sim 12'$ (0.4 pc) from the star. The detected emission shows a "head-tail" morphology, but with complex substructure. Regions with detected H I emission correlate with far-ultraviolet-luminous regions on large scales, but the two tracers are not closely correlated on smaller scales ($\lesssim 1'$). We propose that detectable tails of H I are likely to be a common feature of red giants undergoing mass-loss.

Subject headings: stars: AGB and post-AGB – stars: Individual (Mira AB) — stars: winds, outflows – radio lines: stars

1. Introduction

Mira (*o* Ceti) is a mass-losing star on the asymptotic giant branch (AGB). It is the archetype of a class of pulsating, long-period variables, characterized by regular pulsations (with periods of order hundreds of days) and large-amplitude variations in optical brightness (by up to ∼8 mag; e.g., Reid & Goldston 2002). Mira is also a member of a wind-accreting binary system, Mira AB, with a projected separation of ∼0″.5 (∼54 AU; Matthews & Karovska 2006)[4].

[1]Harvard-Smithsonian Center for Astrophysics, 60 Garden Street, Cambridge, MA, USA 02138

[2]LERMA, UMR 8112, Observatoire de Paris, 61 av. de l'Observatoire, F-75014 Paris, France

[3]GEPI, UMR8111, Observatoire de Paris, 5 Place J. Janssen, F-92195 Meudon Cedex, France

[4]All physical quantities quoted in this paper assume a distance of 107 pc (Knapp et al. 2003).

Despite being the subject of observational scrutiny for many decades, Mira continues to yield surprises. Recently, using far-ultraviolet (FUV) imaging data from the *GALEX* satellite, Martin et al. (2007; hereafter M07) discovered that Mira is surrounded by a bow shock structure and sports a spectacular cometary-like tail, stretching two degrees ($\sim$4 pc) on the sky. Mira has a rather high space velocity [$\sim$128 km s^{-1} with respect to the interstellar medium (ISM); see § 4], and the tail extends backwards along its direction of motion. This tail is believed to arise from the interaction of Mira's wind with the ambient medium as the star moves supersonically through the ISM. The tail is the first of its kind ever discovered, and M07 proposed that its FUV emission arises from H_2 molecules that are collisionally excited by turbulent mixing between the cool molecular gas and the electrons from a shock-heated gas component.

We recently observed Mira in the H I 21-cm line using the Nançay Radio Telescope (NRT) and the Very Large Array (VLA)[5] as part of a larger, ongoing H I survey program of the circumstellar envelopes of evolved stars (see Gérard & Le Bertre 2006; Matthews & Reid 2007). H I is now known to be common in circumstellar environments and frequently shows evidence of extending to very large distances from the star ($\gtrsim$1 pc; Gérard & Le Bertre 2006 and references therein).

Mira was previously observed in H I by Bowers & Knapp (1988), and for more than a decade remained the only AGB star known to have associated H I emission. Unfortunately, the data of Bowers & Knapp had a signal-to-noise too low to permit a detailed investigation of the morphology and kinematics of the circumstellar material, although these authors did report tentative evidence for an interaction between the circumstellar debris and the surrounding ISM. More recently, NRT observations of Mira by Gérard & Le Bertre (2006) provided a significantly improved H I line profile showing a roughly triangular shape, similar to that previously seen in CO (e.g., Winters et al. 2003), as well as evidence for a northward extension of the emission. However, the coarse spatial resolution of the Nançay beam provided little detail on the H I distribution close to the star. To better characterize the extent and morphology of the H I envelope of Mira, we therefore obtained new imaging observations with the VLA. As we describe here, the fortuitous timing of our observations provides a powerful complement to the recent *GALEX* results for understanding the mass-loss history of Mira. To probe the most extended, lowest column density material in the recently discovered FUV tail, we have also obtained new mapping observations of an extended region around Mira using the NRT.

---

[5]The Very Large Array of the National Radio Astronomy Observatory is a facility of the National Science Foundation, operated under cooperative agreement by Associated Universities, Inc.

2. VLA Observations

Mira was observed in the H I 21-cm line with the VLA on 2007 April 1, April 30 and May 11 using the most compact (D) configuration (0.035-1.0 km baselines). This provided sensitivity to emission on scales of up to 15′. The primary beam of the VLA at our observing frequency of ∼1420.3 MHz was ∼ 31′.

The VLA correlator was used in dual polarization (2AC) mode with a 0.78 MHz bandpass, yielding 256 spectral channels with 3.05 kHz (∼0.64 km s^{-1}) spacing. The band was centered at a velocity of 25 km s^{-1} relative to the local standard of rest (LSR); the band center was offset slightly from the systemic velocity of the star ($V_{\rm sys,LSR}$=46.7 km s^{-1}) to avoid placing a strong Galactic feature near the edge of the band.

Observations of Mira were interspersed with observations of two phase calibrators (J0201-115 and J0220-019) approximately every 20 minutes. 3C48 was used as an absolute flux calibrator, and an additional strong point source (J2253+161) was observed as a bandpass calibrator. To insure that the absolute flux scale and bandpass calibration were not corrupted by Galactic emission in the band, the flux and bandpass calibrators were each observed twice, first with the band shifted by +1 MHz and then by −1 MHz, relative to the band center used for the observations of Mira and the phase calibrators. We estimate that this method yields an absolute flux scale accurate to ∼10-15%.

At the time of our observations, the VLA contained 23 working antennas, 9 of which had been retrofitted as part of the Expanded Very Large Array (EVLA) upgrade. In total, 10.25 hours of integration were obtained on Mira. However, some data were lost due to shadowing or hardware problems, and significant flagging to excise radio frequency interference (RFI) was necessary, resulting in a loss of ∼13% of the observed visibilities. During our first observing session, roughly half of the baselines had to be flagged in all channels numbering integral multiples of 12, 13, and 14, owing to a strong local RFI source that emitted an interference "comb". The source of this RFI was identified as the Small Radio Telescope at the VLA Visitor Center, and was switched off during the subsequent two observing sessions.

Our VLA data were calibrated and reduced using the Astronomical Image Processing System (AIPS). To avoid closure errors on VLA-EVLA baselines, we computed and applied a bandpass solution to the raw data before proceeding with any further calibration (G. van Moorsel, private communication). A new frequency-averaged dataset was then computed and used to calibrate the frequency-independent complex gains (see Table 1). Following this, a second correction to the bandpass was computed and applied, and time-dependent frequency shifts were applied to the data to compensate for changes caused by the Earth's motion. Finally, prior to imaging, the u-v data were continuum-subtracted using a linear fit

to the real and imaginary components of the visibilities. Channels 20-85 and 105-160 were determined to be line-free and were used for these fits. These channel ranges correspond to LSR velocities of 52.7−94.6 km s^{-1} and 4.4−39.8 km s^{-1}, respectively. The continuum subtraction procedure was also effective at removing frequency-independent patterns in the channel images caused by solar contamination.

We imaged the VLA line data using the standard AIPS CLEAN deconvolution algorithm and produced data cubes using several different weighting schemes, two of which are presented here (Table 2). We also produced an image of the 21-cm continuum emission in the region using a vector average of the line-free portion of the band.

Table 1. VLA Calibration Sources

Source	α(J2000.0)	δ(J2000.0)	Flux Density (Jy)	Date
3C48[a]	01 37 41.2994	+33 09 35.132	15.88*	All
0201-115[b]	02 01 57.1647	−11 32 31.133	2.64±0.03	2007April1
...	...	...	2.59±0.03	2007April30
...	...	...	2.65±0.04	2007May11
0220-019[b]	02 20 54.2800	−01 56 51.800	3.33±0.06	2007April1
...	...	...	3.33±0.10	2007April30
...	...	...	3.23±0.06	2007May11
2353+161[c]	22 53 57.7479	+16 08 53.560	14.43±0.27†	2007April1
...	...	...	14.29±0.29†	2007April30
...	...	...	14.75±0.08†	2007May11

Note. — Units of right ascension are hours, minutes, and seconds, and units of declination are degrees, arcminutes, and arcseconds.

*Adopted flux density at 1420.3 MHz, computed according to the VLA Calibration Manual (Perley & Taylor 2003).

†Quoted flux density is the mean from the two observed frequencies; see text.

[a]Primary flux calibrator.

[b]Secondary gain calibrator.

[c]Bandpass calibrator.

Table 2. Deconvolved Image Characteristics

Image Descriptor (1)	$\mathcal{R}$ (2)	Taper (kλ,kλ) (3)	$\theta_{\rm FWHM}$ (arcsec) (4)	PA (degrees) (5)	rms (mJy beam^{-1}) (6)
Robust +1	+1	...	$63'' \times 54''$	−3	1.6-2.0
Tapered	+5	2,2	$111'' \times 97''$	+31	1.6-2.1
Continuum	+1	...	$64'' \times 56''$	−10	0.73

Note. — Explanation of columns: (1) image or data cube designation used in the text; (2) robust parameter used in image deconvolution (see Briggs 1995); (3) Gaussian taper applied in u and v directions, expressed as distance to 30% point of Gaussian in units of kilolambda; (4) dimensions of synthesized beam; (5) position angle of synthesized beam (measured east from north); (6) rms noise per channel (1σ; line data) or in frequency-averaged data (continuum).

3. VLA Results

3.1. The Morphology of Mira's H I Envelope and Tail

Figure 1 presents H I total intensity contours for Mira derived from our VLA imaging, overlaid on the *GALEX* FUV image from M07. H I data with velocities from $V_{\rm LSR} = 40.5$ to $V_{\rm LSR} = 50.1$ km s^{-1} were included in these images. To improve signal-to-noise in deriving the H I maps, we rejected pixels in the original data cubes whose absolute values fell below 1.5σ after smoothing spatially with a Gaussian kernel of width 3 pixels ($30''$) and spectrally with a Hanning function.

Our lower resolution H I map (left) reveals a distinct "head-tail" structure, stretching roughly $12'$ ($\sim$0.4 pc) on the sky. [Note that the full extent of the H I is significantly greater than seen here (see § 4), but the VLA is insensitive to the more extended emission.] We see that the brightest H I emission is concentrated near the position of Mira itself. A trail of emission then extends to the northeast, following the same position angle as the FUV tail.

In our higher resolution H I map (Figure 1, right), some fraction of the total emission is lost (as it falls below our rejection threshold), but we see that on smaller scales the H I morphology of Mira becomes clumpy and complex. The location of the peak intensity of the H I emission shows a small but statistically significant offset to the southwest of the star's FUV position: $(\Delta\alpha, \Delta\delta)$=($-12''.1\pm4''.3$,$-14''.5\pm4''.8$). This offset is comparable to the radius of the molecular envelope of Mira found by Josselin et al. (2000)—consistent with the possibility that the bulk of Mira's wind is molecular when it leaves the star, but subsequently is partially dissociated, preferentially in the direction of the leading edge of the shock front. Close to the star, it is clear that the H I emission is not symmetrically distributed about Mira, but exhibits an enhancement to the northwest. An enhancement in K I emission was also seen along this direction by Josselin et al. This type of asymmetry might arise in part from anisotropies in the outflowing wind and/or density gradients in the surrounding ISM (see Vigelius et al. 2007). As the H I emission branches off to the north, it roughly follows a ridge of bright FUV knots (part of what M07 term the "North Stream"), before bifurcating into two lobes. A few additional isolated clumps of H I are also visible to the north.

All of the H I emission detected from Mira with the VLA overlaps with the FUV light seen by *GALEX*, although the detailed relationship between the two tracers is unclear. H I is seen concentrated along the western side of the tail where the FUV emission is also the brightest. However, a significant fraction of the FUV tail shows no H I counterpart, including the bow shock, the southeastern edge of the tail, and the FUV-bright region lying between Mira and the bow shock (termed the "South Stream" by M07). Moreover, on smaller scales there is no obvious correlation between the observed column density of the H I emission and

the surface brightness of the FUV emission. Detection of Hα emission from the UV-bright knots by M07 suggests that most of the gas at these locations is likely to be partially ionized. In the case of the South Stream, given that this region has a different FUV−NUV color than the rest of the tail, the medium here may be very highly ionized, and that the FUV emission from this location may have a different origin (e.g., hot plasma emission).

3.2. The Velocity Structure of the H I Emission Surrounding Mira

Individual H I channel maps from our VLA imaging observations are shown in Figure 2. We find that near the position of the star, the emission detected in the central velocity maps (44.3-47.5 km s^{-1}) has a larger spatial extent than in the outer velocity channels, as would be expected for an expanding envelope. At the same time, several of the channels show additional emission extending toward the North that arises from the near-tail. The velocity field of the latter component appears complex, suggesting that the small-scale motions of the tail gas may be affected by turbulence. This is consistent with the interpretation of the tail as a turbulent wake (e.g., Wareing et al. 2007b).

Figure 3 shows the global H I spectrum of Mira derived from the VLA observations. The spectrum shown as a thick black line was derived from the "Tapered" data cube (Table 2) by summing all emission within a 8′(E-W)×13.′6(N-S) box centered at $\alpha_{J2000.0} = 2^{\rm h}\ 19^{\rm m}\ 22.8^{\rm s}$, $\delta_{J2000.0} = -2^\circ\ 54'\ 9''$. Uncertainties on the total flux densities in each channel are $\sim \pm 0.01$ Jy. The VLA H I profile agrees well with the NRT line profile derived toward Mira and is discussed further in § 5.1.

3.3. Detection of H I Absorption in the Tail

The 21-cm continuum emission within a 30′ region surrounding Mira comprises a number of weak point sources with a total observed flux density of ∼0.4 Jy (uncorrected for primary beam attenuation). Mira AB itself is undetected, and we detect no continuum emission coincident with any of the bright knots seen in the UV and in Hα by M07. The brightest continuum source in the region lies at $\alpha_{\rm J2000.0} = 02^{\rm h}\ 19^{\rm m}\ 07.36^{\rm s}$, $\delta_{\rm J2000.0} = -02^\circ\ 52'\ 49.''2$, and we measure for it a flux density of 0.228±0.003 Jy (after correction for the primary beam). It overlaps with the FUV emission detected by *GALEX*, but lies outside the region where H I was detected in emission with the VLA. We have examined a spectrum toward this source and detect a weak ($\sim 3\sigma$) absorption feature (Figure 4). Based on a Gaussian fit, this feature has a peak flux density $S_0 = -6.1 \pm 1.9$ mJy, a FWHM of $\Delta v = 7.1 \pm 0.9$ km s^{-1},

and a central velocity $V_{\rm LSR} = 44.7 \pm 0.9$ km s^{-1}. Both the central velocity and the width of the line feature are consistent with the H I gas observed in the tail of Mira in emission (see Figures 3 and 5).

Detection of H I in absorption in the tail of Mira allows us to obtain a constraint on the spin temperature of the gas. For the "Robust +1" data, the limiting H I column density for a detection of H I in *emission*, integrated over a Gaussian line profile with FWHM 7.1 km s^{-1}, is $N_{\rm HI} \lesssim 1.3 \times 10^{19}$ cm^{-2} (3σ). Under the assumption that the absorbing gas at the position of the continuum source has an equal or lower column density than gas detected in emission, one may then write:

$$T_s \leq \frac{N_{\rm HI}}{(1.8 \times 10^{18}) \int \tau(v) dv} \ {\rm K} \tag{1}$$

where T_s is the spin temperature of the atomic hydrogen and τ is its optical depth (e.g., Dickey et al. 1978). The assumption of a Gaussian line shape yields a line-integrated optical depth for the H I absorption profile of $\approx$0.20, and therefore $T_s \lesssim 37$ K. Clumping of the absorbing material would further reduce this limit, implying that a component of the tail gas is rather cool.

4. Observations with the Nançay Radio Telescope

To achieve greater sensitivity to extended, low surface brightness H I emission in the vicinity of Mira, we made observations at several positions along its tail with the NRT (see Table 3). Our pointings were selected using the *GALEX* map from M07 as a guide. These observations were obtained between 2007 September and 2007 December as part of a Target of Opportunity program.

The NRT is a meridian-transit-type telescope with an effective collecting area of roughly 4000 m^2. At 1420 MHz, its half-power beam width is $4'$ in right ascension and $22'$ in declination for a source at the declination of Mira (-2°). Typical system temperatures are $\sim$35 K. Further properties of the NRT are described in van Driel et al. (1997). The large collecting area of the NRT and the good match between the N-S extension of the beam and the direction of Mira's wake make the NRT well-suited to searching for extended, low column density material.

Our observational strategy for mapping the tail consisted of position-switched measurements at each pointing, with beam-throws of $\pm 12'$ or $\pm 16'$ in the E-W direction. One-third of the time was devoted to the on-position and two-thirds of the time to the off-source comparison spectra. A full NRT spectrum has a bandwidth of 165 km s^{-1} and a spectral resolution of 0.08 km s^{-1}. A total of 44 hours of data were obtained along the tail. Fortunately, there

is minimal Galactic H I emission near the LSR velocity of Mira; this provides flat baselines that permit us to detect weak signals efficiently. Data processing was performed using the CLASS software and consisted of subtracting a linear baseline from each spectrum before averaging.

The results of our NRT mapping are summarized in Table 3, and we show a sampling of our spectra in Figure 5. We have clearly detected H I emission from Mira's tail as far as 88′ north of the star. Moreover, we see the peak velocity of the emission becomes progressively blueshifted with increasing distance from the star, indicating an overall deceleration (see also § 5.2). We did not detect H I in any of the NRT pointings that have no overlap with Mira's FUV tail, consistent with the material giving rise to the FUV light and the H I being spatially coupled along the full length of the tail.

Table 3. NRT Mapping of Mira's Tail

Position offset:[a] (arcmin E, arcmin N)	Integration time (hours)	rms noise (mJy)	Velocity (km s^{-1})	Line width (km s^{-1})	$F_{\rm peak}$ (mJy)
(0,0)	49	4.56	45.4±0.5	7.1±0.3	42.51±0.46
(0,+22)	4	8.85	...	...	...
(+4,+22)	7	5.78	41.2±0.5	7.3±1.2	11.6±1.7
(+8,+22)	2	10.30	...	...	...
(+8,+44)	7	6.42	38.9±0.5	8.4±1.1	15.2±1.7
(+12,+66)	4	7.64	...	...	...
(+16,+66)	4	11.10	32.4±0.9	9.3±2.1	14.7±2.9
(+18,+88)	4	11.30	...	...	...
(+20,+88)	4	9.04	...	...	...
(+24,+88)	4	9.19	27.7±0.7	8.4±1.6	13.9±2.3
(+24,+110)	4	9.11	...	...	...

Note. — Tabulated line parameters are derived from Gaussian fits to the spectra shown in Figure 5.

[a]The adopted coordinates of Mira were $\alpha_{J2000.0}$=$02^{\rm h}$ $19^{\rm m}$ $20.79^{\rm s}$, $\delta_{J2000.0}$=-02° $58'$ $39''.51$.

5. Results and Interpretation

5.1. The Global H I Line Profile and Total H I Mass of Mira's Circumstellar Material

The region near the position of Mira has been extensively observed with the NRT since 2000 (see also Gérard & Le Bertre 2006). The H I line spectrum we derive by integrating the emission throughout a $12(\text{E-W})' \times 22'(\text{N-S})$ region agrees well with the integrated line profile obtained with the VLA (Figure 3). Based on Gaussian fits to the global line profiles from the two telescopes, we find line centroids of 45.69±0.20 km s^{-1} and 45.41±0.26 km s^{-1} for the NRT and VLA, respectively. These centroids are slightly blueshifted compared with the value derived from CO(2-1) line observations by Winters et al. (2003; $V_{\rm CO} = 46.7 \pm 0.3$ km s^{-1}). We note however that the CO line is somewhat asymmetric and appears to be comprised of multiple components. Based on a two-component fit to the CO(3-2) spectrum, Knapp et al. (1998) find the broader component to be slightly blueshifted ($V_{\rm CO} = 46.0$±1.0 km s^{-1}), making it consistent with the H I centroid to within uncertainties. The FWHM of the H I profiles are 6.64±0.20 km s^{-1} (NRT) and 6.13±0.26 km s^{-1} (VLA), comparable to linewidths measured from CO data (Knapp et al. 1998; Winters et al. 2003). However, whereas the CO linewidths directly gauge the expansion velocity of the stellar wind, the H I profile width may be affected by turbulent motions in the tail gas (§ 3.2) or by possible thermal broadening (Libert et al. 2007).

Integrating over the line profiles shown in Figure 3 yields integrated flux densities of 0.47±0.04 Jy km s^{-1} (VLA) and 0.51±0.03 Jy km s^{-1} (NRT). Assuming the H I is optically thin, the total H I mass contained within the portion of the circumstellar material imaged by the VLA is $M_{\rm HI} \approx 1.27(\pm 0.13) \times 10^{-3}\ M_\odot$. Using the NRT measurements summarized in Table 3, we can also estimate the additional amount of atomic material in the extended tail to be $M_{\rm HI} \sim 2.7 \times 10^{-3}\ M_\odot$. (Here we have multiplied the observed emission by a geometric correction factor of 2 to account for the fact that we have not fully sampled the tail). The combined H I mass for the circumstellar envelope and tail of Mira is then $M_{\rm HI} \sim 4 \times 10^{-3}\ M_\odot$.

5.2. A Revised Age for Mira's Tail

A key result of our NRT mapping is that the spectra reveal a clear slowing-down of the material in the tail with increasing distance from Mira (Table 3 and Figure 5). At ∼1°.5 from the star, the peak H I signal is ∼14 mJy, with $V_{\rm LSR} = 27.7 \pm 0.7$ km s^{-1}, whereas the centroid of the H I signal at the center position is 45.4±0.5 km s^{-1}. This finding is consistent with the model of Wareing et al. (2007b), who predicted an increasing velocity lag with respect

to the velocity of Mira itself with increasing distance along the tail. This result also implies that the tail is older than the age of 3×10^4 years derived by M07 under the assumption that this material is stationary with respect to the ISM.

From Table 3, we can extrapolate to estimate the radial velocity of the H I material at 2° from Mira (i.e., at the most extreme position where *GALEX* detected emission) to be $V_{\rm LSR} \sim 23 \pm 3$ km s^{-1}. Adopting the stellar radial velocity determined from CO observations ($V_{\rm LSR}$ =46.7 km s^{-1}; Winters et al. 2003), the proper motion from Perryman et al. (1997), and the solar motion parameters from Dehnen & Binney (1998), we estimate Mira's velocity in the plane of the sky, corrected for solar motion, to be $V_t \approx$120 km s^{-1}. The velocity lag for the outermost tail material is therefore 23±3 km s^{-1} in the radial direction and $\sim$ 61.0±7.7 km s^{-1} in the plane of the sky. Finally, assuming a uniform deceleration of the stellar gas, we derive an age of $t \sim (1.20^{+0.17}_{-0.14}) \times 10^5$ years for the material detected by *GALEX* at 2° from Mira. This calculation does not take into account a possible variation of the mass-loss rate or the turbulence of the interstellar medium that the stellar gas may encounter.

Our age estimate for Mira's tail exceeds previous observational estimates for Mira's total mass-loss duration by roughly an order of magnitude or more (see Young et al. 1993; Bowers & Knapp 1988; Gérard & Le Bertre 2006; M07). Furthermore, the tail age approaches the expected interval between two thermal pulses; the relatively modest change in surface brightness over the length of Mira's tail then suggests that the predicted growth in the mass-loss rate for AGB stars between thermal pulses (e.g., Vassiliadis & Wood 1993) may be smaller than previously assumed.

5.3. Comments on the Composition of Mira's Circumstellar Envelope and Tail

Adopting the mass-loss rate for Mira derived from CO observations ($\dot{M} \sim 1.7\times10^{-7}$ $M_\odot$ yr^{-1}; Ryde & Schöier 2001) and assuming this mass-loss rate has remained constant in time, the age derived in § 5.2 implies that the total mass of Mira's circumstellar debris should be $\sim 2.0 \times 10^{-2}$ $M_\odot$. After adjusting our current H I measurements for the mass of He, we then estimate that neutral atomic material accounts for ∼25% of Mira's circumstellar envelope and tail. We now briefly comment on some possible implications of this finding.

Previous observations have shown that Mira's wind is likely to be predominantly molecular as it leaves the star (e.g., Bowers & Knapp 1988; Josselin et al. 2000; Wood et al. 2002). However, as discussed by Josselin et al., the bulk of Mira's circumstellar material is expected to be dissociated by the interstellar radiation field at radii of $r \gtrsim 2 \times 10^{16}$ cm from

the star. Therefore, unless the wind is very clumpy (thereby increasing the survival time of the molecules), it is expected that atomic matter will comprise a significant fraction of the material that is ultimately swept by ram pressure into the tail.

Under the assumption that the FUV light from Mira's tail arises entirely from collisional excitation of H_2 by hot electrons (M07), an expected by-product will be rapid dissociation of molecules (see also Raymond et al. 1997), thus providing an additional atomic contribution to Mira's tail. Indeed, the dissociation rate of $\sim 2.5 \times 10^{42}$ s^{-1} assumed by M07 should have produced roughly a factor of four more H atoms during the past 1.2×10^5 years than we observe. Assuming some fraction of the wind is atomic before being swept into the tail, this raises some difficulty in how to maintain a sufficient supply of H_2 to power Mira's FUV luminosity over its inferred lifetime. A significantly lower molecular dissociation rate ($\sim$10%) could help resolve this problem; however such a rate approaches that expected from the interstellar radiation field alone (Morris & Jura 1983). If a portion of the material in Mira's tail is clumpy, self-shielding of the molecular hydrogen could also help to increase its lifetime (see, e.g., Huggins et al. 2002). A search for CO emission associated with such a clumped component in Mira's tail would be of considerable interest. An alternative explanation may be that some fraction of the FUV light from Mira's tail arises from processes involving atomic material, such as the H two-photon continuum (e.g., D'Odorico et al. 1980) and/or bremsstrahlung emission from a hot ($T \sim 10^5$ K) "surface" of the tail. Future multi-wavelength observations and modelling should help to clarify these issues.

6. Discussion: Are H I Tails Ubiquitous Features of Evolved Stars Undergoing Mass-Loss?

We have reported the detection of an extended tail of neutral, atomic hydrogen associated with the AGB star Mira. This H I 21-cm line emission arising from the tail coincides with the FUV-luminous wake recently discovered by M07. Although Mira is currently the only known star to have a FUV-bright tail, we draw attention to the possibility that its H I tail may represent an extreme example of a rather common phenomenon for evolved stars undergoing mass-loss.

Gérard & Le Bertre (2006) already reported evidence that H I emission associated with circumstellar envelopes may be offset from the position of the central star. In addition, Matthews & Reid (2007) previously reported the detection of an H I "plume" stretching $\sim$0.2 pc from the semi-regular variable star RS Cnc. We have since confirmed that the geometry of this plume is consistent with material trailing the motion of RS Cnc through the ISM. More recently, we have imaged an analogous, but somewhat shorter tail associated with

another semi-regular variable star, X Her (Gardan et al. 2006; Matthews et al., in prep.). Both of these stars have smaller space velocities than Mira ($\sim$18 km s^{-1} and $\sim$100 km s^{-1}, respectively), indicating that unusually high space motion is not a prerequisite for tail formation; indeed, it may require only that the stellar space velocity exceeds the expansion velocity of the wind.

While the sample of stars imaged in H I is presently small, evidence of interaction between the circumstellar envelope and the ISM has also been seen in the global H I spectra of a number of H I-detected stars (e.g., Gérard & Le Bertre 2006 and references therein). Observed H I line profile shapes are frequently inconsistent with a classic spherically symmetric model of mass-loss at a constant outflow speed, and may show velocity centroids offset from those observed in CO. As shown by Gardan et al. (2006) and Libert et al. (2007), these profiles can be well reproduced once the effects of ISM interaction are accounted for. The importance of ISM interactions in the evolution of circumstellar envelopes has also been underscored by the numerical simulations of Villaver et al. (2002) and Wareing et al. (2007a,c), and by the discovery of a far-infrared bow shock associated with the AGB star R Hya (Ueta et al. 2006). *We therefore propose that extended gaseous tails may be ubiquitous features of evolved stars undergoing mass-loss.* For stars with low space velocities, hot companions[6], and/or largely atomic winds, these tails may lack associated bow shock structures and/or a detectable FUV counterpart, but should in many instances be readily detectable via H I 21-cm line observations. The conditions for detection of these tails will be most favorable for stars at high Galactic latitudes and/or with systemic velocities well removed from those of the bulk of the Galactic emission.

We thank R. Perley and the VLA staff for tracking down the RFI problem affecting our early observations. We are also grateful to M. Seibert for providing us with the *GALEX* FUV image and to J. Raymond for valuable discussions. The Nançay Radio Observatory is the Unité Scientifique Nançay of the Observatoire de Paris and is associated with the French Centre National de Recherche Scientifique (CNRS) as the Unité de Service et de Recherche (USR), No. B704. The Observatory also gratefully acknowledges the financial support of the Région Centre in France. The VLA observations presented here were part of program AM887.

[6]Mira's hot companion, Mira B, is unlikely to significantly affect the composition of Mira's wind and tail owing to the small extent of the ionized zone surrounding it (see Matthews & Karovska 2006).

REFERENCES

Bowers, P. F. & Knapp, G. R. 1988, ApJ, 332, 299

Briggs, D. S. 1995, Ph.D. Thesis, New Mexico Institute of Mining and Technology (http://www.aoc.nrao.edu/ftp/dissertations/dbriggs/diss.html)

Dehnen, W. & Binney, J. 1998, MNRAS, 298, 387

Dickey, J. M., Terzian, Y., & Salpeter, E. E. 1978, ApJS, 36, 77

D'Odorico, S., Benvenuti, P., Dennefeld, M., Dopita, M. A., & Greve, A. 1980, A&A, 92, 22

Gardan, E., Gérard, E., & Le Bertre, T. 2006, MNRAS, 365, 245

Gérard, E. & Le Bertre, T. 2006, AJ, 132, 2566

Huggins, P. J., Forveille, T., Bachiller, R., Cox, P., Ageorges, N., & Walsh, J. R. 2002, ApJ, 573, L55

Josselin, E., Mauron, N., Planesas, P., & Bachiller, R. 2000, A&A, 362, 255

Knapp, G. R., Pourbaix, D., Platais, I., & Jorissen, A. 2003, A&A, 403, 993

Knapp, G. R., Young, K., Lee, E., & Jorissen, A. 1998, ApJS, 117, 209

Libert, Y., Gérard, E., & Le Bertre, T. 2007, MNRAS, 380, 1161

Martin, D. C. et al. 2007, Nature, 448, 780 (M07)

Matthews, L. D. & Karovska, M. 2006, ApJ, 637, L49

Matthews, L. D. & Reid, M. J. 2007, AJ, 133, 2291

Morris, M. & Jura, M. 1983, ApJ, 264, 546

Perley, R. A. & Taylor, G. B. 2003, VLA Calibration Manual (http://www.vla.nrao.edu/astro/calib/manual/index.shtml)

Raymond, J. C., Blair, W. P., & Long, K. S. 1997, ApJ, 489, 314

Reid, M. J. & Goldston, J. E. 2001, ApJ, 568, 931

Ryde, N. & Schöier, F. L. 2001, ApJ, 547, 384

Ueta, T. et al. 2006, ApJ, 648, L39

van Driel, W., Pezzani, J., & Gérard, E. 1997, in High-Sensitivity Radio Astronomy, ed. R. J. Davis and N. Jackson, (Cambridge: Cambridge University Press), 229

Vassiliadis, E. & Wood, P. R. 1993, ApJ, 413, 641

Vigelius, M., Melatos, A., Chatterjee, S., Gaensler, B. M., & Ghavamian, P. 2007, MNRAS, 374, 793

Villaver, E., García-Segura, G., & Manchado, A. 2002, ApJ, 571, 880

Wareing, C. J., Zijlstra, A. A., & O'Brien, T. J. 2007a, ApJ, 660, L129

Wareing, C. J., Zijlstra, A. A., O'Brien, T. J., Seibert, M. 2007b, ApJ 670, L125

Wareing, C. J., Zijlstra, A. A., & O'Brien, T. J. 2007c, MNRAS, 382, 1233

Winters, J. M., Le Bertre, T., Jeong, K. S., Nyman, L.-Å., & Epchtein, N. 2003, A&A, 409, 715

Wood, B. E., Karovska, M., & Raymond, J. C. 2002, ApJ, 575, 1057

Young, K., Phillips, T. G., & Knapp, G. R. 1993, ApJ, 409, 725

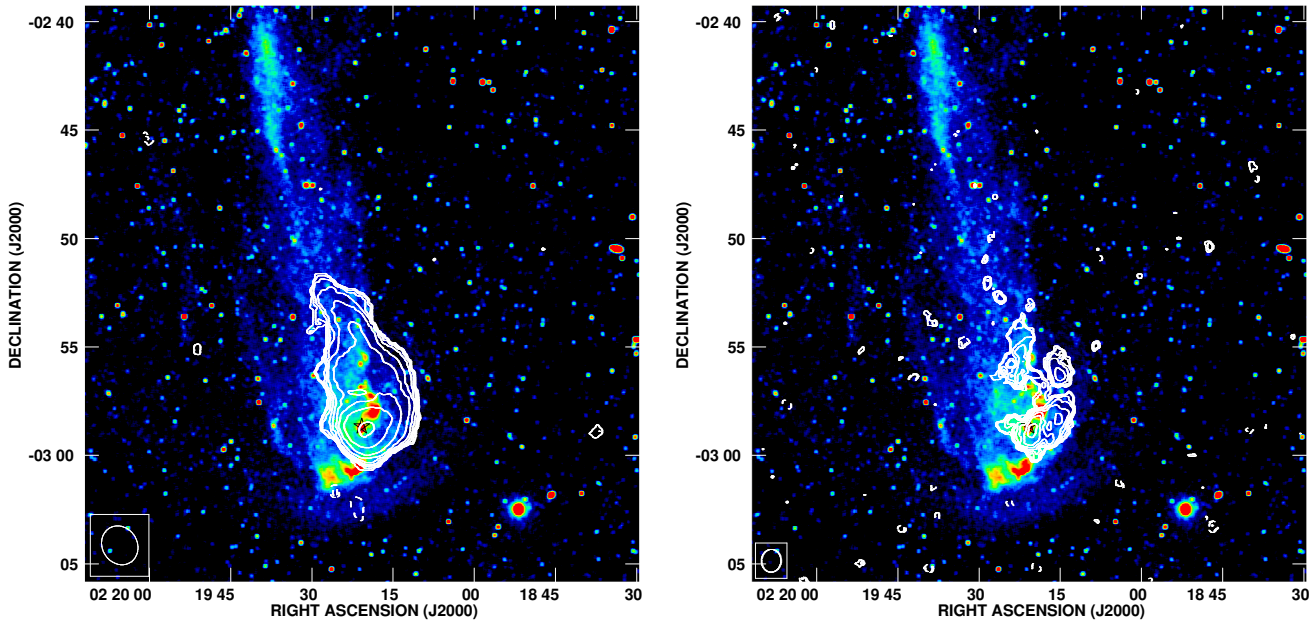

Fig. 1.— H I total intensity contours overlaid on false color *GALEX* FUV images of Mira from M07. The *GALEX* image has been smoothed with a 3×3 pixel (4.″5×4.″5) boxcar function. The full extent of the FUV emission is not shown. The left panel shows the H I contours derived from the "Tapered" image while the right panel shows those from the "Robust +1" image (see Table 2). Contour levels are $(-2, 1.4, -1, 1, 1.4, 2, ...22.4) \times 3.5$ Jy beam^{-1} m s^{-1} (left); $(-2, -1.4, 1.4, 2, ...11.2) \times 3.5$ Jy beam^{-1} m s^{-1} (right). A black star symbol designates the position of Mira ($\alpha_{J2000.0}$=02$^{\rm h}$ 19$^{\rm m}$ 20.79$^{\rm s}$, $\delta_{J2000.0}$=−02° 58′ 39.″51).

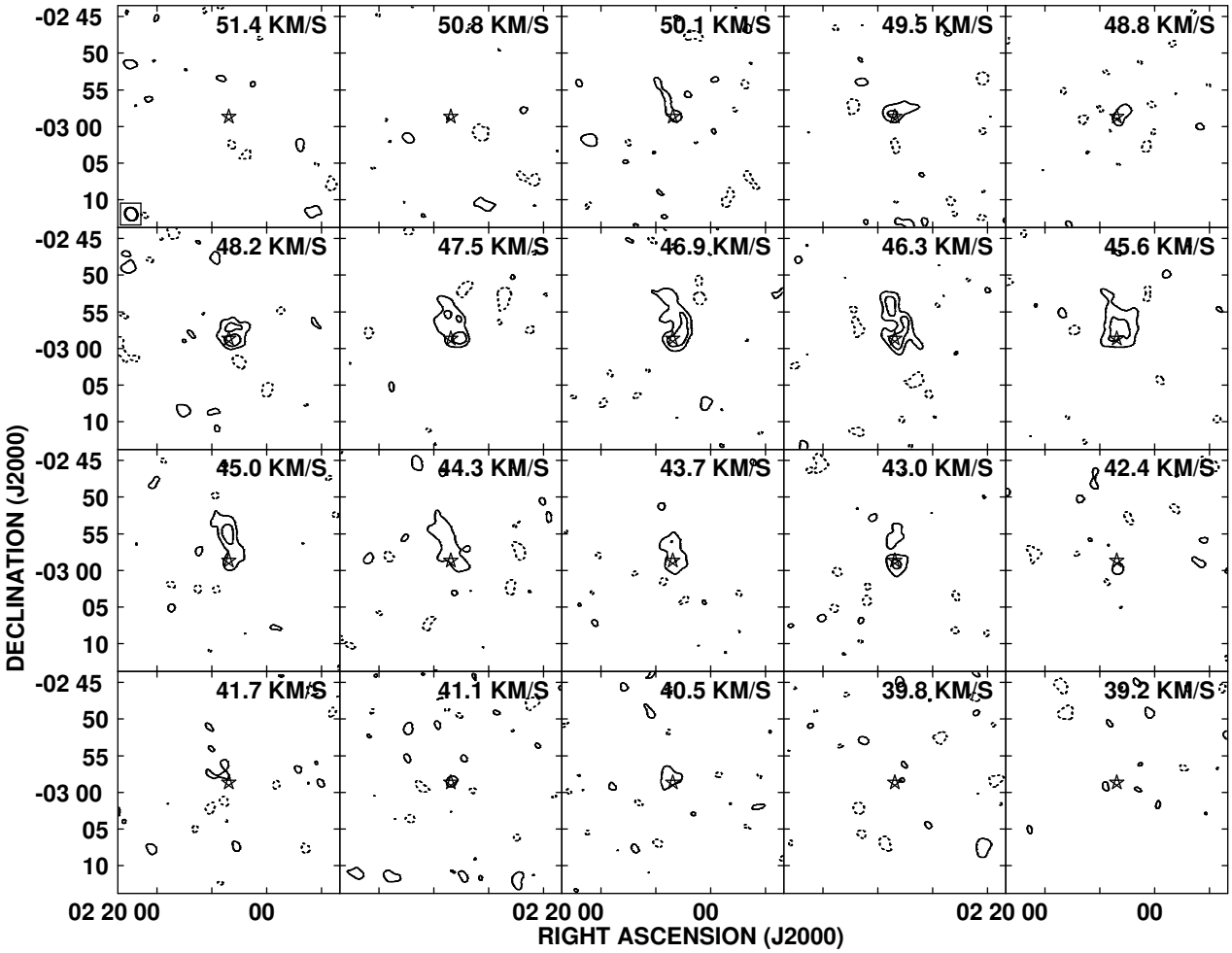

Fig. 2.— H I channel maps near the systemic velocity of Mira, taken from the VLA "Tapered" data cube (Table 2). Contour levels are $(-5[\text{absent}], -2.5, 2.5, 5) \times 1.8$ mJy beam^{-1}. A star symbol indicates the position of Mira.

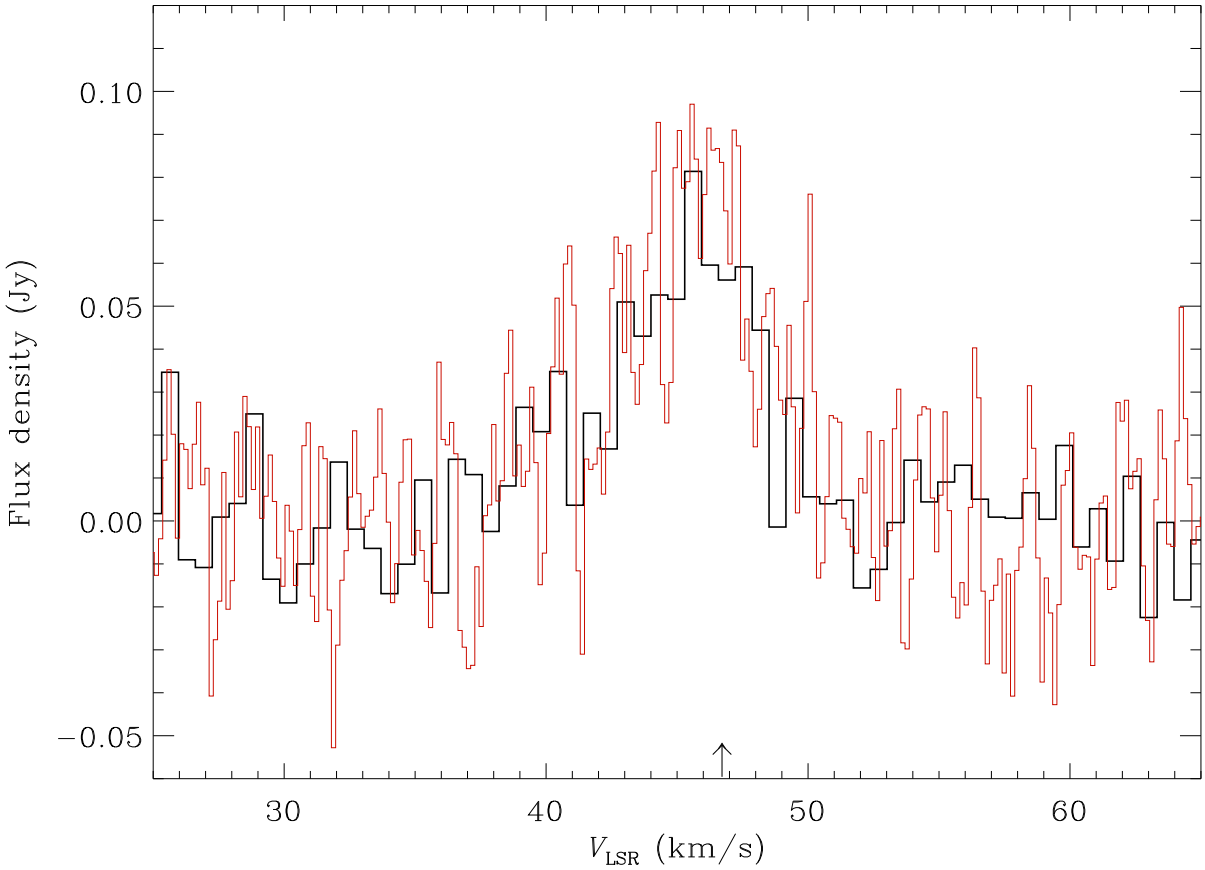

Fig. 3.— H I spectra toward Mira. The thin red line shows the NRT spectrum obtained by summing the measurements over a 12(E-W)′ × 22′(N-S) region; the thick black line shows the VLA spectrum obtained by summing within a 8.′0×13.′6 region. The arrow indicates the stellar systemic velocity obtained from CO observations by Winters et al. 2003.

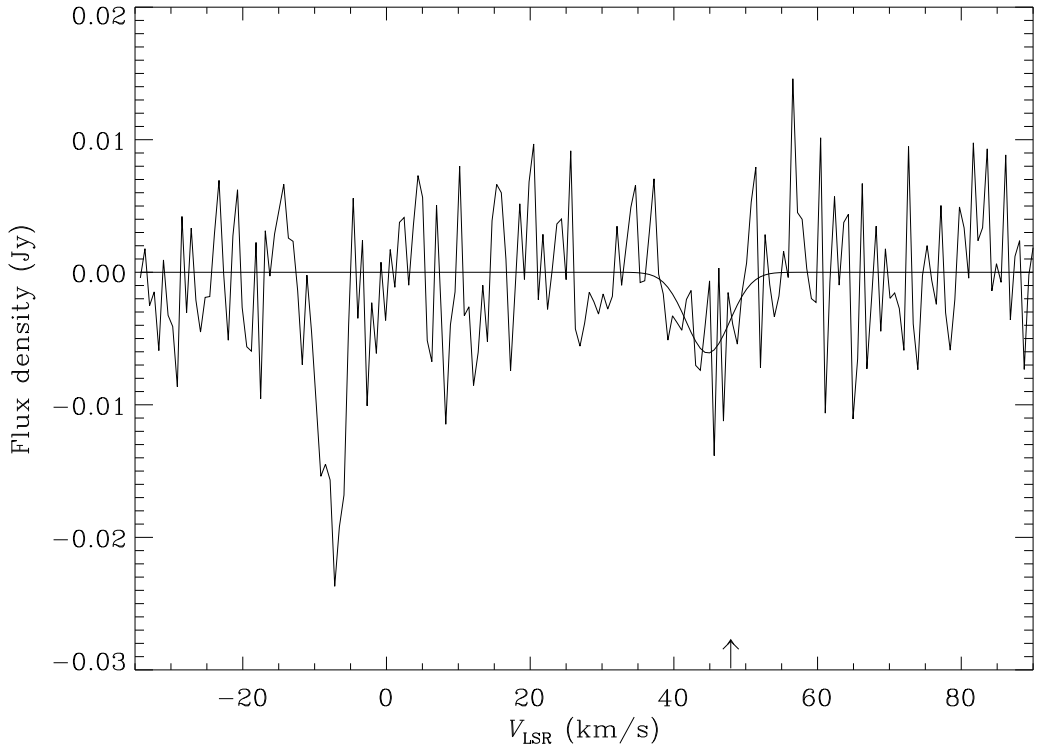

Fig. 4.— H I absorption spectrum toward the continuum source at $\alpha_{\rm J2000.0} = 02^h19^m07.35^s$, $\delta_{\rm J2000.0} = -02°52'49''.8$. The flux from the continuum source itself has been subtracted. The stronger, blueshifted absorption feature near -8 km s^{-1} is due to Galactic interstellar material along the line-of-sight, but the weaker, redshifted feature has a velocity and linewidth consistent with the circumstellar material surrounding Mira. The thick line shows a Gaussian fit to the latter feature (see text for details). An arrow indicates the stellar systemic velocity of Mira determined from CO observations.

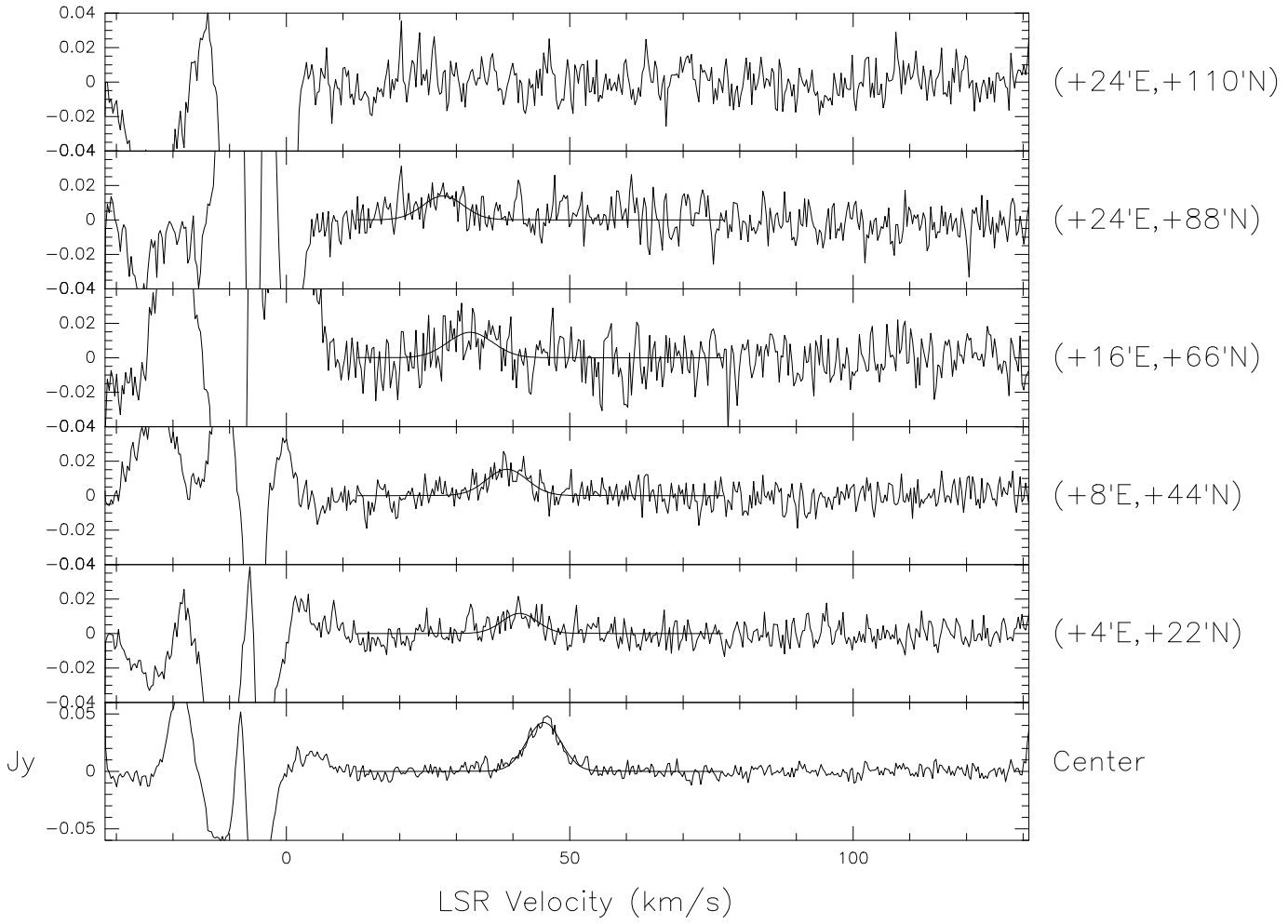

Fig. 5.— NRT H I spectra along Mira's tail. The spectra shown have been smoothed to a velocity resolution of 0.32 km s^{-1}. Gaussian fits to the emission from Mira are overplotted. Note the bottom panel has a different vertical scale. Features blueward of $V_{\rm LSR}$ ≈10 km s^{-1} are from intervening Galactic emission.